*Korean J. Chem. Eng.*, **26**(5), 1383-1388 (2009)
DOI: 10.1007/s11814-009-0218-3

# Sorption kinetics of carbon dioxide onto rubidium carbonate

**Kyu-Suk Hwang*, Sang-Wook Park*,†, Dae-Won Park*, Kwang-Joong Oh*, and Seong-Soo Kim****

*Division of Chemical Engineering, Pusan National University, Busan 609-735, Korea
**School of Environmental Science, Catholic University of Pusan, Busan 609-757, Korea
(*Received 11 February 2009 • accepted 3 March 2009*)

**Abstract**−Rubidium carbonate was used as an adsorbent to capture carbon dioxide from gaseous stream of carbon dioxide, nitrogen, and moisture in a fixed-bed to obtain the breakthrough data of $CO_2$. Experiments were carried out at flow rates of carbon dioxide and nitrogen ($5\times10^{-6}$-$35\times10^{-6}$ $m^3$/min), moisture ($0.5\times10^{-6}$-$3.0\times10^{-6}$ $m^3$/h), amount of adsorbent ($0.5\times10^{-3}$-$1.8\times10^{-3}$ kg), mole fraction of carbon dioxide (0.03-0.22), and different sorption temperatures (323-353 K) at atmospheric pressure. The deactivation model in the non-catalytic heterogeneous reaction systems was used to analyze the sorption kinetics among carbon dioxide, carbonate, and moisture, employing the experimental breakthrough data that fit the deactivation model better than the adsorption isotherm models in the literature.

Key words: Carbon Dioxide, Sorption, Breakthrough Curve, Deactivation Model, Rubidium Carbonate

## INTRODUCTION

Carbon dioxide ($CO_2$) produced by combustion of fossil fuels is regarded as the most significant greenhouse gas with its increasing accumulation in the atmosphere attracting worldwide attention [1]. Various methods have been used to remove it: absorption by solvent and adsorption by molecular sieve, membrane separation, and cryogenic fractionation. In particular, absorption has been widely used in the chemical industries, as with the Benfield Process [2]. Another technique is dry scrubbing or sorption of $CO_2$ onto an alkaline metal carbonate as a solid adsorbent. This is a modified hybrid technology of adsorption and chemical absorption with the advantage of being a simple and convenient operation for separation and recovery of $CO_2$ in flue gases. The development of alkaline metal carbonates, such as an alumina gel [3], alumina [4], activated carbon [5-7], and silica/alumina vermiculite [8], is the focus of the current study to improve the sorption efficiency of the carbonate.

The carbonation reaction mechanism of alkaline metal carbonate by $CO_2$ under moist conditions to form alkali metal bicarbonate was verified by x-ray diffraction [5-7] and SEM imaging of patterns on the solid surface [5-11]. But the stoichiometric coefficient of $H_2O$ in the carbonation reaction between alkali metal carbonate, $CO_2$, and moisture depends on the type of carbonates [10] of anhydrate and hydrate, as well as the kind of alkaline metal, Li, Na, K, Rb, and Cs [5-11]. Most studies for $CO_2$ capture by alkaline metal carbonate have been carried out in a fixed-bed, but a thermogravimetric analyzer [12,13] has been used to get an initial rate of carbonation for the sorption kinetics of $CO_2$.

In mass transfer processes that accompany chemical reactions, such as a non-catalytic heterogeneous gas-solid reaction [14-18], the diffusion may have an effect on the reaction kinetics [19]. It is difficult and tedious to analyze the adsorption breakthrough curve using conventional isotherm models [20,21], such as the Langmuir, Freundlich, Brunauer-Emmett-Teller (BET), and Dubinin-Radushkevich-Kagener (DRK) models, and prepare the experimental values of the sorption isotherm with a reasonable diffusivity [22] of a solute. Conversely, the deactivation model (DM) [23,24], as a simplified model, has been used to predict the breakthrough curve, assuming that the formation of a dense product layer over the surface of the adsorbent changed the number of active sites and the possible variations in the adsorption of active sites to cause a drop in the adsorption rate. Suyadal et al. [25] presented adsorption kinetics of trichloroethylene vapor on activated carbon using breakthrough curves by DM and assumed that the adsorption kinetics of DM were first-order with respect to organic vapor and zero$^{th}$ order with respect to activity of the adsorbent, respectively, but, not first-order with respect to activity of the adsorbent. Park et al. have successfully applied DM for carbonation of sodium carbonate [26], potassium carbonate [27] with $CO_2$, and adsorption of toluene vapor onto activated carbon [28] and have indicated DM described gas-solid noncatalytic reactions more accurately than the unreacted core and volume reaction models, using deactivation kinetics with first-order with respect to the solid carbonate and the $CO_2$ concentration, respectively. Rubidium carbonate was used as an adsorbent in this study, which is one of the series of works to investigate the sorption kinetics from analysis of the breakthrough data by DM.

## THEORY

Anhydrous rubidium carbonate reacts with $CO_2$ and moisture to form rubidium bicarbonate by the following equation:

$$Rb_2CO_3(s)+CO_2(g)+H_2O(g)\rightarrow 2RbHCO_3(s) \qquad \text{(i)}$$

The reaction (i) is a non-catalytic heterogeneous gas-solid reaction. The mathematical analysis of this heterogeneous process must take into account the simultaneous influence of reaction and of heat and mass transfer to predict the conversion as a function of time for a solid undergoing reaction. To obtain the kinetics of the reaction (i) using $CO_2$ breakthrough data, the deactivation model is used as

†To whom correspondence should be addressed.
E-mail: swpark@pusan.ac.kr

follows.

The formation of a dense product layer over the adsorbent creates an additional diffusion resistance and is expected to cause a drop in the adsorption rate. One would also expect it to cause significant changes in the accessible pore volume, active surface area, and activity per unit area of the adsorbent with respect to the extent of the adsorption. All of these changes cause a decrease of vacant surface area of the adsorbent with time. In DM, the effects of all of these factors on the diminishing rate of $CO_2$ capture are combined in a deactivation rate term.

With assumptions [28] of the pseudo-steady state and the isothermal species, the conservation equation of $CO_2$ in the fixed bed is as follows:

$$-Q_g\frac{dC_A}{dS}-kC_A\alpha=0 \tag{1}$$

In writing this equation, axial dispersion in the fixed bed and any mass transfer resistances are assumed to be negligible. According to the proposed DM [29], the rate of change of the activity of the adsorbent is expressed as:

$$-\frac{d\alpha}{dt}=k_dC_A^n\alpha^m \tag{2}$$

The zero$^{th}$ solution of DM is obtained by taking n=0 and m=1 with the initial activity of the solid as unity:

$$a(t)=\exp[-k\tau\exp(-k_dt)] \tag{3}$$

Eq. (3) is identical to the breakthrough equation proposed by Suyadal et al. [25] and assumes a fluid phase concentration that is independent of deactivation processes along with the adsorbent. More realistically, one would expect the deactivation rate to be concentration-dependent and, accordingly, axial-position-dependent in the fixed bed.

To obtain the analytical solution of Eq. (1) and (2) by taking n=m=1, an iterative procedure is applied. The procedure used here is similar to the paper proposed by Dogu [29] for the approximate solution of nonlinear equations. In this paper, the zero$^{th}$ solution (Eq. (3)) is substituted into Eq. (2), and the first correction for the activity is obtained by the integration of this equation. The corrected activity expression is then substituted into Eq. (1), and integration of this equation gives the first corrected solution for the breakthrough curve:

$$a(t)=\exp\left[\frac{[1-\exp(k\tau(1-\exp(-k_dt)))]}{1-\exp(-k_dt)}\exp(-k_dt)\right] \tag{4}$$

This iterative procedure can be repeated for further improvement of the solution. In this procedure, higher-order terms in the series solutions of the integrals are neglected. The breakthrough curve for DM with two parameters (k and $k_d$) is calculated from the concentration profiles by Eq. (4).

## EXPERIMENTAL

Rubidium carbonate was a reagent grade (Aldrich Chemicals, 99.8%) of non-porous material [26] and used after washing with acetone and drying. The size of adsorbent particle was measured in the range of 0.075-0.85 mm using a sieve analyzer (Sam Jin Co. Ltd.) to obtain the surface area of the adsorbent and its density was the value from its maker. Porosity of the fixed bed was measured by a conventional method [28] using a mass cylinder. The values of $d_p$, $\rho_B$, and $f_{bed}$ were 345.2 μm, 1,552 kg/m$^3$ and 0.76, respectively The surface area of the particles was calculated with mean size and density of the particle, and its value was 2.80 m$^2$/kg.

To obtain the breakthrough curves of $CO_2$, the sorption experiments were carried out in the presence of carbon dioxide and moisture with rubidium carbonate adsorbent in a fixed bed pyrex glass reactor (inside diameter=2 cm) in a range of 5-35 cm$^3$/min of the gaseous flow rate ($Q_g$) of $CO_2$ and $N_2$, 0.03-0.22 mole fraction ($y_A$) of $CO_2$, 0.5-3.0 cm$^3$/h of the moisture flow rate ($Q_w$), 0.5-1.8 g of the adsorbent ($w_o$), temperature range of 323-358 K at atmospheric pressure. Heated water vapor was fed to the reactor through the line by using a micro syringe. Each experiment was duplicated at least once under identical conditions. A gas chromatograph (detector; thermal conductivity detector, column; Haysep D (10 feet by 1/8 inch of stainless steel, detector temperature, 190 (±0.1) °C; feed temperature, 160 (±0.1) °C; flow rate of He, 25.7 cm$^3$/min, retention time of $N_2$, $CO_2$, $H_2O$: 0.9, 1.323, 20.6 min) was connected to the exit stream of the reactor for the on-line analysis of $CO_2$, $N_2$, and water vapor. The amount of gaseous mixture entering from the reactor to the automatic sampler of GC was 2 cm$^3$, and the oven temperature in the GC was constant as 160 (±0.1) °C. The fixed bed reactor and the experimental procedure were identical to those previously reported [26].

## RESULTS AND DISCUSSION

The sorption kinetics of $CO_2$ on $Rb_2CO_3$ using two parameters of DM were investigated by using the breakthrough curves of $CO_2$, measured according to the changes of the experimental variables such as $Q_g$, $Q_w$, $w_o$, and sorption temperature as follows:

### 1. Effect of the Flow Rate of Gaseous Mixture of $CO_2$ and $N_2$

To investigate the effect of $Q_g$ on the kinetics, the breakthrough curves of $CO_2$ were measured in a range of 7-23 cm$^3$/min of $Q_g$ at

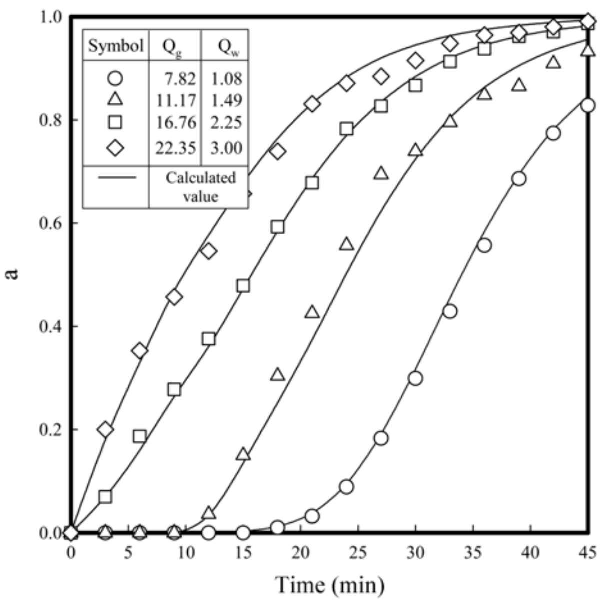


**Fig. 1. Effect of the flow rate of mixture of $N_2$ and $CO_2$ on the breakthrough curves of $CO_2$ at $w_o$=1.5 g and 60 °C.**

**Table 1. Rate parameters for various experimental conditions at 60 °C**

| $Q_g$ ($cm^3$/min) | $Q_w$ ($cm^3$/h) | $w_o$ (g) | $y_A$ (-) | k×$10^3$ ($m^3/m^2$·min) | $k_d$ ($m^3$/kmol·min) | $r^2$ |
|---|---|---|---|---|---|---|
| 7.82 | 1.08 | 1.5 | 0.118 | 8.741 | 0.1321 | 0.9992 |
| 11.17 | 1.49 | 1.5 | 0.115 | 8.643 | 0.1337 | 0.9937 |
| 16.76 | 2.25 | 1.5 | 0.116 | 8.773 | 0.1308 | 0.9995 |
| 22.35 | 3.0 | 1.5 | 0.116 | 8.572 | 0.1355 | 0.9967 |
| 33.64 | 0.6 | 1.5 | 0.038 | 8.475 | 0.1314 | 0.9927 |
| 23.58 | 1.0 | 1.5 | 0.055 | 8.843 | 0.1383 | 0.9969 |
| 5.81 | 1.7 | 1.5 | 0.219 | 8.956 | 0.1336 | 0.9997 |

$y_A$=0.115 before adding water, 1-3 $cm^3$/h of $Q_w$, $w_o$=1.5 g, and 60 °C. Because concentrations of $CO_2$ and water vapor at the inlet of the column depended on $Q_g$ and $Q_w$, $Q_w$ being fed into the micro syringe were controlled by using the mass balance for three components. The measured values of breakthrough curves of $CO_2$ were plotted against sorption time with parameters of $Q_g$ and $Q_w$ as various symbols in Fig. 1.

As shown in Fig. 1, a shift of breakthrough curves to smaller times was observed with an increased $Q_g$, with a decrease in sorption capacity, indicating that the sorption conversion decreases as the space-time of the gaseous mixtures in the fixed bed, i.e., the sorption time decreases. Analysis of the experimental breakthrough data by a nonlinear least squares technique was in agreement with Eq. (4). The evaluated values of k and $k_d$ are listed in Table 1, and calculated curves using Eq. (4) are shown in Fig. 1 as solid lines with a correlation coefficient ($r^2$) of more than 0.993. As shown in Table 1, the values of k and $k_d$ are nearly identical.

**2. Effect of the Flow Rate of Water**

To observe the effect of $Q_w$ on the kinetics, the breakthrough curves of $CO_2$ were measured in a range of 0.6-3.0 $cm^3$/h of $Q_w$, 5-34 $cm^3$/min of $Q_g$, 0.03-0.22 of $y_A$, $w_o$=1.5 g, and 60 °C. $Q_g$ and $y_A$ were adjusted according to the change of $Q_w$ in order that the concentration of $CO_2$ at the inlet of the column may be the same as mentioned above. The measured values of breakthrough curves of $CO_2$ were plotted against the sorption time with parameters of $Q_w$, $Q_g$ and $y_A$ as various symbols in Fig. 2.

As shown in Fig. 2, the sorption capacity of $CO_2$ increases with increasing $Q_w$, indicating that the sorption conversion increases as the concentration of reactant (water) increases. The values of k and $k_d$ were evaluated with the same procedure mentioned above and listed in Table 1. The calculated curves using Eq. (4) are shown in Fig. 2 as solid lines with $r^2$ more than 0.992. As shown in Table 1, the values of k and $k_d$ are nearly identical.

**3. Dependence of the Kinetics on the Sorption Temperature**

To determine the dependence of the kinetics on the sorption temperature, the breakthrough curves of $CO_2$ were measured in the temperature range between 50 and 80 °C at $Q_g$=11.17 $cm^3$/min, $Q_w$=1.49 $cm^3$/h, $y_A$=0.115, and $w_o$=1.5 g. The values of k and $k_d$ were evaluated from the analysis of the experimental breakthrough data by a nonlinear least squares technique along the same procedure mentioned above, with the Arrhenius plots shown in Fig. 3 satisfying the linear relationship.

Using the values of slope and intercept of these straight lines, the activation energy of sorption and deactivation of $Rb_2CO_3$ are 19.9 and 51.4 kJ/gmol, respectively, and the empirical equations

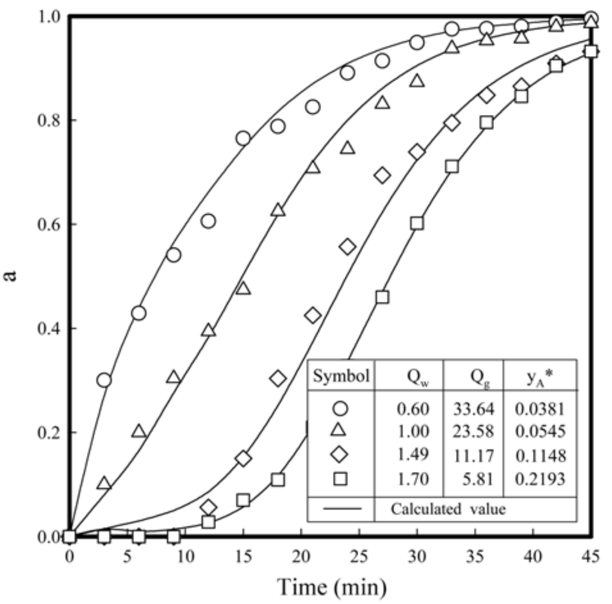


**Fig. 2. Effect of the flow rate of water on the breakthrough curves of $CO_2$ at $w_o$=1.5 g and 60 °C.**

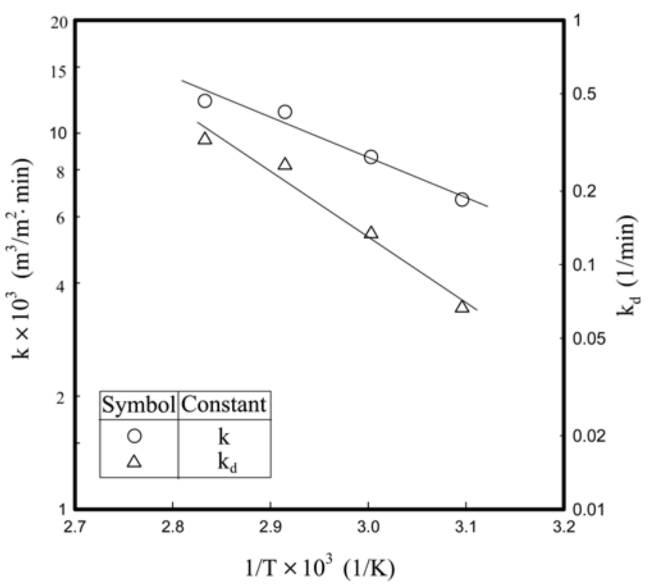


**Fig. 3. Arrhenius plots of k and $k_d$ at $Q_g$=11.17 $cm^3$/min, $Q_w$=1.49 $cm^3$/h, and $w_o$=1.5 g.**

**Table 2. Selected sorption isotherms to fit the breakthrough data of $CO_2$ for comparison with the deactivation model**

| Adsorption isotherms | Mathematical representation of adsorption isotherms | Linearized forms | Parameters and correlation coefficient ($r^2$) |
|---|---|---|---|
| Langmuir | $y=\frac{ax}{(1+bx)}$ | $\frac{1}{y}=\frac{1}{ax}+\frac{b}{a}$ | $a=9.042\times10^3$<br>$b=1.898\times10^4$<br>$r^2=0.3858$ |
| Freundlich | $y=ax^b$ | $\ln(y)=\ln(a)+b\ln(x)$ | $a=0.8007$<br>$b=0.1848$<br>$r^2=0.8573$ |
| Brunauer-Emmett-Teller | $y=\frac{x}{(1-x)(a+bx)}$ | $\frac{x}{y(1-x)}=a+bx$ | $a=-42.17$<br>$b=312.7$<br>$r^2=0.2217$ |
| Dubinin-Radushkevich-Kagener | $y=a\exp[-b\ln^2(x)]$ | $\ln(y)=\ln(a)-b\ln^2(x)$ | $a=0.6383$<br>$b=0.0154$<br>$r^2=0.6283$ |
| Deactivation model (this study) | x according to Eq. (7)<br>y according to Eq. (8) | | $k\tau=2.9708$<br>$k_d=0.1337$<br>$r^2=0.9999$ |

are as follows:

$$k=11.261\exp\left(-\frac{19.9}{RT}\right) \tag{5}$$

$$k_d=1.457\times10^3\exp\left(-\frac{51.4}{RT}\right) \tag{6}$$

## 4. Comparison of the Proposed Models

Several equilibrium models [20,21], developed to describe sorption isotherm relationships, are useful for describing sorption capacity and theoretical evaluation of thermodynamic parameters, such as heats of sorption. Sometimes, the experimental procedure to prepare the sorption isotherm relationships is very tedious and requires excessive time. Suyadal et al. [25] used the breakthrough data for comparison of DM with sorption isotherms such as models listed in Table 2 as follows:

The equilibrium concentrations between two phases, used to describe sorption isotherm relationships, can be obtained by Eqs. (7) and (8), where a(t), x, and y are the dimensionless concentrations of $CO_2$ in the breakthrough data, in the gas phase and solid phase, respectively:

$$x=\frac{\int_0^t a(t)dt}{\int_0^\infty a(t)dt} \tag{7}$$

$$y=\frac{t-x\int_0^\infty a(t)dt}{\int_0^\infty dt-x\int_0^\infty a(t)dt} \tag{8}$$

where x, and y are the dimensionless concentrations of $CO_2$ in the gas phase through the sorption isotherm and solid phase, respectively:

As shown in Eqs. (7) and (8), the ranges of x and y are between 0 and 1, respectively. The equilibriums for single-solute sorption given in the literature [20,21] are frequently presented as dimensionless concentration isotherms.

To compare the deactivation model with the equilibrium isotherms, the typical experimental conditions, indicated with the triangle, in Fig. 2, were used as $Q_g$=11.17 cm$^3$/min, $Q_w$=1.49 cm$^3$/h, $y_A$=0.115, $w_o$=1.5 g, and 60 °C. The values of a(t), obtained from the breakthrough curves of $CO_2$, x, and y, estimated by Eq. (7) and (8), are shown in Fig. 4 and used to obtain the constants of a and b in each model.

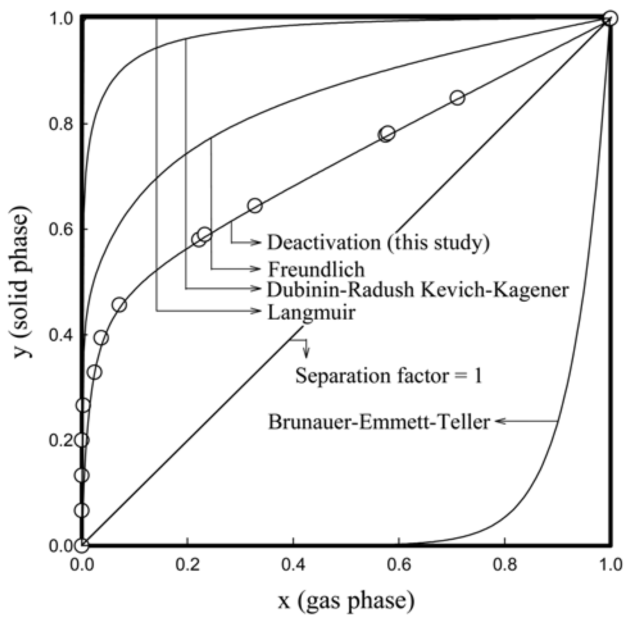


**Fig. 4. Comparisons of the model in describing the experimental breakthrough curve of $CO_2$ according to Table 2.**

As shown in Table 2 and Fig. 4 the proposed deactivation model fit the data with the highest $r^2$ of 0.9999, and the sorption of $CO_2$ on the adsorbent might be favorable isotherms due to the separation factor being less than unity. The Brunauer-Emmett-Teller (BET) model is an extended model of Langmuir and includes multi-layer sorption phenomena. BET has a few assumptions: any given layer need not be completed before subsequent layers can form, the first layer of molecules adheres to the surface with a comparable energy to the heat of sorption for monolayer attachment, and subsequent

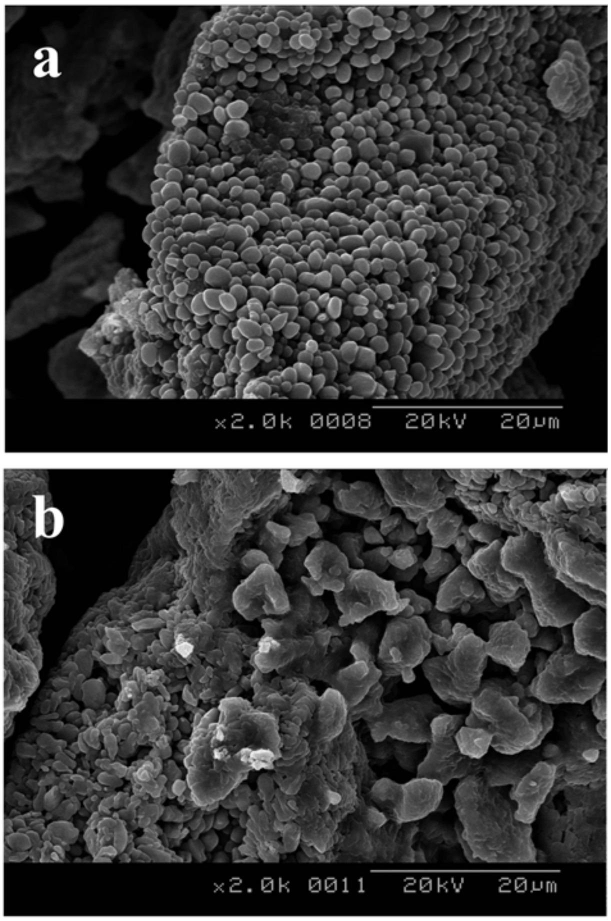


**Fig. 5. SEM image patterns of the surface of the solid (a: $Rb_2CO_3$; b: product of $Rb_2CO_3$ carbonation).**

layers are essentially condensation reactions [24]. Failure of the BET model in the fitting with the experimental data in Fig. 5 may be explained by the fact that the practical sorption situation between the $CO_2$ and adsorbent used in this study may be different from that of the BET model, and that the multi-layer sorption phenomena do not occur in our study.

Fig. 5(a) shows the surface pattern (SEM) of anhydrous $Rb_2CO_3$, the reactant for all of the experimental runs. A uniform pore structure of small size is observable in the material. Fig. 5(b) illustrates the product formed during the typical reaction time of 45 minutes.

The surface pattern of the product is different from that of the reactant. The product could potentially consist of $Rb_2CO_3$ and $RbHCO_3$, although we could not obtain the $RbHCO_3$ sample from a manufacturer. It can be concluded that the deactivation model with two parameters can be used to analyze the breakthrough data of $CO_2$ in the fixed bed because changes in the pore structure causes significant variations in the carbonation rates and the reactivity of the reactant from the results of Fig. 6.

## CONCLUSIONS

The breakthrough data of $CO_2$ were measured in a fixed bed to observe the sorption kinetics of $CO_2$ onto rubidium carbonate with moisture under the following experimental conditions: flow rate of gaseous mixture at 5-35 $cm^3$/min, flow rate of water at 1-3 $cm^3$/h, amount of rubidium carbonate at 0.5-2 g, and sorption temperature of 50-80 °C. A high degree of correlation was achieved between the deactivation model and the experimental breakthrough data in the heterogeneous solid-gas reaction system with changes in the pore structure and the reactivity of the solid reactant. The sorption rate constant and the deactivation rate constant were evaluated by analysis of the experimental breakthrough data using a nonlinear least squares technique, and described as Arrhenius forms. The experimental breakthrough data fit better to the deactivation model than the sorption isotherm models in the literature.

## ACKNOWLEDGMENTS

This work was supported by Brain Korea 21 Project and a grant (2006-C-CD-11-P-03-0-000-2007) from Energy Technology R&D of Korea Energy Management Corporation. Dae-Won Park is also thankful for KOSEF (R01-2007-000-10183-0).

## NOMENCLATURE

a : dimensionless concentration ($C_A/C_{Ao}$) of $CO_2$ in the breakthrough data
$C_i$ : concentration of species, i in bulk phase [kmol/$m^3$]
$d_p$ : diameter of the adsorbent [m]
$f_{bed}$ : porosity of the fixed bed
k : initial second-order sorption rate constant [$m^3/m^2\cdot$min]
$k_d$ : deactivation rate constant at n=0 [1/min], or n=1 [$m^3$/kmol·min]
$Q_g$ : volumetric flow rate of gaseous mixture [$m^3$/min]
$Q_w$ : volumetric flow rate of water [$m^3$/hr]
$r^2$ : correlation coefficient
S : vacant surface area of the adsorbent [$m^2$]
t : sorption time [min]
T : sorption temperature [K]
$w_o$ : amount of the adsorbent [kg]
x : dimensionless concentrations of $CO_2$ in the gas phase through the sorption isotherm
y : dimensionless concentrations of $CO_2$ in the solid phase through the sorption isotherm
$y_A$ : mole fraction of $CO_2$ in feed gas mixture
$y_A^*$ : mole fraction of $CO_2$ with moisture free in feed gas mixture

### Greek Letters

$\alpha$ : activity of the adsorbent
$\rho$ : density of the adsorbent [kg/$m^3$]
$\tau$ : surface time as initial vacant surface area of the adsorbent to $Q_o$ [min/m]

### Subscripts

A : $CO_2$
o : initial value
w : moisture

## REFERENCES

1. M. Aresta, *Carbon dioxide recovery and utilization*, Kluwer Aca-

demic Pub., Boston (2003).
2. R. K. Bartoo, *Chem. Eng. Prog*., **80**, 35 (1984).
3. W. Fuchs and N. T. Syosett, US Patent 3,511,595 (1970).
4. D. Gidaspow and M. Onischak, US Patent 3,865,924 (1975).
5. S. Hirano, N. Shigomoto, S. Yamada and H. Hayashi, *Bull. Chem. Soc. Jpn*., **68**, 1030 (1995).
6. H. Hayashi, H. J. Taniuchi, N. Furuyashiki, S. Sugiyama, S. Hirano, N. Shigemoto and T. Nonaka, *Ind. Eng. Chem. Res*., **37**, 185 (1998).
7. T. Shigemoto, S. Sugiyama and H. Hayashi, *J. Chem. Eng. Jpn*., **38**, 711 (2005).
8. A. G. Okunev, V. E. Sharnov, Y. I. Aristov and V. N. Parmon, *React. Kinet. Catal. Lett*., **71**, 355 (2004).
9. M. C. Ball, A. N. Strachan and R. M. Strachan, *J. Chem. Faraday, Trans*., **87**, 1911(1991).
10. M. C. Ball, R. A. Clarke and A. N. Strachan, *J. Chem. Faraday, Trans*., **87**, 3683 (1991).
11. M. C. Ball, C. M. Snelling, A. N. Strachan and R. M. Strachan, *J. Chem. Faraday, Trans*., **88**, 631 (1992).
12. J. S. Hoffman and H. W. Pennline, *J. Energy & Environ. Res*., **1**, 90 (2001).
13. D. A. Green, B. S. Turk, R. P. Gupta, W. J. McMichael, D. P. Harrison and Y. Liang, *Quarterly technical progress report*, Louisiana State University, January (2003).
14. L. K. Doraiswamy and M. M. Sharma, *Heterogeneous reactions*, vol. 1, John Wiley & Sons, Inc., New York (1984).
15. M. Ishida and C. Y. Wen, *AIChE J*., **14**, 311 (1968).
16. P. A. Ramachandran and B. D. Kulkarni, *Ind. Eng. Chem. Res. Process Des. Dev*., **19**, 717 (1980).
17. J. W. Evans and S. Song, *Ind. Eng. Chem. Process Des. Dev*., **13**, 146 (1974).
18. B. S. Sampath, P. A. Ramachandran and R. Hughes, *Chem. Eng. Sci*., **30**, 135 (1975).
19. M. G. Ranade and J. W. Evans, *Ind. Eng. Chem. Process Des. Dev*., **19**, 118 (1980).
20. D. W. Ruthven, *Principles of adsorption and adsorption processes*, John & Wiley, New York (1984).
21. M. Suzuki, *Adsorption engineering*, Kodansga Ltd., Tokyo (1990).
22. N. Orbey, G. Dogu and T. Dogu, *Can. J. Chem. Eng*., **60**, 314 (1982).
23. S. Yasyerli, T. Dogu, G. Dogu and I. Ar, *Chem. Eng. Sci*., **51**, 2523 (1996).
24. T. Kopac and S. Kocabas, *Chem. Eng. Comm*., **190**, 1041 (2003).
25. Y. Suyadal, M. Erol and M. Oguz, *Ind. Eng. Chem. Res*., **39**, 7249 (2000).
26. S. W. Park, D. H. Sung B. S. Choi and K. W. Oh, *Sep. Sci. Technol*., **41**, 2665 (2006).
27. S. W. Park, D. H. Sung, B. S. Choi, J. W. Lee and H. Kumazawa, *J. Ind. Eng. Chem*., **12**, 522 (2006).
28. S. W. Park, B. S. Choi and J. W. Lee, *Sep. Sci. Technol*., **42**, 2221 (2007).
29. T. Dogu, *AIChE J*., **32**, 849 (1986).